ALBORÁN BASIN, SOUTHERN SPAIN-PART I: GEOMORPHOLOGY

Muñoz, A.[a], Ballesteros, M.[b], Montoya, I.[c], Rivera, J.[b], Acosta, J.[b], Uchupi, E.[d]

[a] Secretaría General de Pesca Marítima, Corazón de María, 8, 28002 Madrid, Spain

[b] Instituto Español de Oceanografía, Corazón de María, 8, 28002 Madrid, Spain

[c] Universidad Juan Carlos I, Campus de Móstoles, Madrid, Spain

[d] Woods Hole Oceanographic Institution, Woods Hole, MA 02543, USA

ABSTRACT

Bathymetric, 3D relief and shaded relief maps created from multibeam echo-sounding data image the morphology of the Alborán Basin, a structural low along the east–west-trending Eurasian–African plates boundary. Topographic features in the basin are the consequence of volcanism associated with Miocene rifting, rift and post-rift sedimentation, and recent faulting resulting from the convergence of the African–Eurasian plates. Pleistiocene glacially induced regressions/transgressions when the sea level dropped to about 150 m below its present level gas seeps and bottom currents. Recent faulting and the Pleistocene transgressions/regressions led to mass- wasting, formation of turbidity currents and canyon erosion on the basin's slopes. Recent fault traces at the base of the northern basin slope have also served as passageways for thermogenic methane, the oxidation of which by bacteria led to the formation of carbonate mounds along the fault intercepts on the sea floor. Expulsion of thermogenic or biogenic gas has led to the formation of pockmarks; erosion by bottom currents has resulted in the formation of moats around seamounts and erosion of the seafloor of the Alborán Ridge and kept the southern edge of the 36º10'N high sediment free.

Keywords: Alborán Basin; Carbonate caps; Carbonate hydrothermal mounds; Mass-wasting; Multibeam bathymetry; Pockmarks; Seamounts; Submarine canyons

1.INTRODUCTION

In this paper, we use multibeam echo sounding data supplemented by a few selected high-resolution topo- graphic parametric system (TOPAS) seismic reflection profiles to define the geomorphology of the marine east–west-trending Alborán Basin, east of the Strait of Gibraltar. The tectonic processes responsible for the creation of this basin are discussed in a companion paper (Ballesteros et al., in press). Here too we discuss the numerous investigations on the offshore and onshore geology carried out in the Alborán Basin and vicinity prior to our investigation. The basin is a 150 km wide and 350 km long structure located within the Alpine orogen off southern Spain and northern Morocco (Fig. 1). It is aligned along the African/Eurasian convergent plate boundary, is underlain by a thin continental crust, has a Neogene- Quaternary rift and post-rift sediment fill that is as much as 7 km thick in several depocenters, and rift-associated Miocene volcanic fill (Comas et al., 1992).

[FIGURE 1]

The present survey of the Alborán Basin took place in 2002 and 2003 during cruises ‘‘500 Viviendas’’, Alborán-02 and Alborán-03 aboard the R/V Vizconde de Eza. These surveys were carried out using a Simrad EM 300 multi- beam echosounder in conjunction with GPSD and inertial aided system (Seapath 200). Multibeam data acquisition was performed using a PC and the data were stored on a CD and displayed in analog form in a line scan EPC recorder. Processing of the multibeam data began with the Neptune program that corrected vessel position along the survey tracks followed by a batch process to eliminate depth records that exceeds twice the standard deviation of the soundings contained in a determinate area. After this, manual editing deleted spurious data in a correlation plot. Clean and consistent digital data triplets (x, y, z) were used by Cfloor software to generate regular grids and establish the desired projection. Cfloor grid was used to elaborate bathymetric maps, DTMs and 3D schemes of the seafloor. High-resolution

seismic reflection investigation of the acoustic stratigraphy of the Alborán Basin was carried out with a TOPAS. The system consists of a hull of transducers in 4 rows with 16 sections, with each row being electronically stabilized for roll, pitch and heave. Operation depths are from 30 m to full ocean depths, with the ship's speed being around 10 knots (16 km/h). The availability of such database on a large segment of the Alborán Basin allows us to appreciate the geomorphology of the basin and ascertain the roles that different geological processes have played in its creation.

2.GEOMORPHOLOGY OF THE ALBORÁN BASIN

2.1. Terminology

As the Alborán Basin is on continental crust, we have avoided the use of such physiographic terms as continental shelf, slope and rise, as they are inappropriate for such a topographic feature. Instead, we deem it more accurate to describe the basin's second-order topographic forms as basin shelf, basin slope and basin apron similar to the terminology used by Emery (1960) for the basins in the Continental Borderland off southern California. In contrast to the basins off southern California, no area within the Alborán Basin is flat enough to be considered a basin plain (marine plains have been defined as surfaces having slopes of less than 1:1000 or 0°03.5'; Heezen et al., 1959), so no such feature is described below. We also restrict the term basin to the Alborán Basin and use the term 'sub-basin' for the lows within the Alborán Basin.

2.2. Northern shelf

The area of the Alborán Basin studied during the present investigation extends from 35º40'N to 36º50'N and from about 2º07'W to 4º40'W (Figs. 2 and 3). As shown by these figures, the Alborán Basin northern shelf west of Adra is about 18 km wide. In the embayment off Malaga, however, the platform widens to 27 km. South of the Campo de Dalías, the shelf displays a maximum width of 23 km narrowing northeastward to about 17 km in the vicinity of Roquetas del Mar. It again widens to 22 km off Almeria and maintains this width to Cabo de Gata, where the shelf, in the shape of a broad north–south trending platform, widens to 28 km (Fig. 2). Little

information was obtained during the present study on the third-order morphological features scarring the shelf's surface, but where the data do extend onto the shelf its surface is cut by normal faults trending obliquely to the shelf's edge. The shelf's edge is generally at a depth of about 100–125 m, but off the Cabo it is at a depth of 175–200 m (Fig. 2). The shelf's edge displays two basic forms, a broad shoulder where the shelf merges gradually with the basin's slope and an abrupt termination marked by a low relief steep scarp oriented obliquely to the shelf's edge. The first is a reflection of sediment deposition and the second of faulting.

[FIGURE 2]

The inner shelf west of the Cabo de Gata platform is mantled by thickening upward and outward prograding units emplaced during the last 6500 years over the Holocene transgressive erosional surface (Ercilla et al., 1992; Hernández-Molina et al., 1996). On mid-shelf, the transgressive unconformity is exposed or thinly covered. Exposures along the coast indicate that the platform off Cabo de Gata consists of Neogene volcanics. The Quaternary sediments covering this volcanic terrain consist of Pleistocene regressive and transgressive facies (Medialdea Vega et al., 1982).

2.3. Northern basin slope

The Alborán Basin northern slope west of Roquetas de Mar is made of two segments, an upper 1–4.5 km wide upper segment extending from the shelf's edge to a depth of approximately 150–200 m, and a more gentler lower one extending from a depth of 150 to 200 to 600 m (Figs. 2 and 3). The gradient of the upper segment ranges from 5º to as high as 10–14º and its relief from 47 to 90 m off the Campo de Dalías, 32–50 m from Campo de Dalías to Adra and 78 to 157 m east of Adra. As illustrated by Ercilla et al. (1992) and Hernández-Molina et al. (1996), part of the outer shelf-upper slope represents the topset/ foreset surfaces of shelf-edge wedges that were emplaced during the last transgression that began about 18,000–20,000 years ago. Other segments of the upper slope, the steeper sections, are exposed sections of a fault line scarp. From Roquetas del Mar to Cabo de Gata in western Almería Bay, the basin slope is continuous from the shelf's edge at a depth of about 100 m to 1300–1400 m, trends east–northeast, is cut by numerous canyons

and channels, and is bordered on the southeast side by the northeast–southwest-oriented Almería Canyon. South of the platform off Cabo de Gata, the slope again consists of two sections, with the upper one having a gradient of 5–14º and extending from a depth of 175–200 to 400 m.

West of Melicena at 3º15'W, the lower slope segment extending to a depth of 600 m is 22 km wide off Malaga, but only 7.5 km east of Almería. The gradient of the lower segment ranges from 3º to 1º. On the east side of the Bay of Almería, southwest of Cabo de Gata, the lower basin slope consists of two topographic elements. The upper one extends from the base of the upper slope at a depth of 400 m to about 700 m with a gradient of 1–3º. On this upper segment are four west of north to north-oriented highs, including the flat-topped Sabinar and Pollux banks. The lower segment extending from 700 to 1600 m has a gradient of 10–14º. Southwest of Sabinar and Pollux banks, this segment is orientated northeast–southwest, but south of the banks it trends east–west. In contrast to the smooth lower slope west of Almería Bay, canyons/channels and broad embayments suggestive of mass-wasting incise the lower slope in Almería Bay and off Cabo de Gata.

[FIGURE 3]

2.4. North basin apron and Djibouti Trough

The north basin apron of the Alborán Basin is divisible into three parts. West of 4ºW, where the West Alborán sub-basin is located, the apron descends gradually south- ward to a depth of 800 m with a gradient of about 1º (Figs. 2 and 3). From 800 m to a depth of 1000 m, the apron's gradient increases to about 2º. Between 1000 and 1200 m its declivity increases progressively to 4º and thence decreases again to less than 1º to a depth of 1500 m. The 1350 m contour defines a low in the apron, oriented west–east, open eastward toward the Alborán Channel. This low is cut into two by a >1350 m deep swell extending northward from B/O (Buque/Oceanografico) Vizconde de Eza Seamount (Fig. 2). The segment of the West Alborán sub-basin imaged in Fig. 2 is 50 km wide, 85 km long and has a maximum depth of >1500 m. Its floor has a slope of about 1º1. East of the basin is the northeast–southwest- trending Alborán Ridge.

On the basin apron east of 3º50'W is a broad embayment (3°25–3°12′W) curving gently to the northeast that has topographic expression to the shelf's edge. Its outer end is at a depth of 850 m and its inner one at a depth of 100 m. Along the east side of the embayment is a southeast to east

of south-plunging swell extending from the shelf's edge to a depth of 850 m; Chella Bank is located east of the axis of this swell (Fig. 2). Along the west side of this swell is a chain of narrow depressions that terminate northward on a line of northwest-trending ridges that in turn terminate about a northeast-aligned fracture (Fig. 3). In its center is another north-trending swell whose outer edge is about 900 m deep. West of the embayment is a northwest to southeast-trending swell at whose southeastern end is the Algarrobo Seamount. This swell marks the location of Malaga sub-basin (Fig. 2). The Alborán Basin north apron from slightly east of 3°50′W to slightly west of 2°45′W, the Motril sub-basin, is dominated by an east–west-aligned trough (we have tentatively named this feature the Djibouti Trough; Fig. 2). The Djibouti Trough is bound on its south side by a border fault located along the northern edge of the 36°10′N high (Watts et al., 1993). The trough, defined by the 850 m contour, trends east–west in its central part between 3°45′W and 3°10′W, and slightly southwest in the west part as it is constrained by two seamounts. The Djibouti Trough has a width of 6–16 km, is approximately 43 km long, and deepens eastward. Its western end is topographically smooth, but its eastern end is deeply embayed.

The Djibouti Trough terminates west and east on outward-facing slopes with a relief of 300 m on the west and 700 m on the east. The 300 m high west slope descending to the West Alborán sub-basin has a gradient 3–1° and the 700 m high east slope descending to the East Alborán sub-basin has a gradient of 6–14°. The East Alborán sub-basin, east of the Djibouti Trough and between the basin's north slope and the Habibas Escarpment, is 35 km wide and 62 km long and has a maximum depth of >1975 m. Its seafloor has a slope of about 1°. Flanking the sub-basin in the west is the Alborán Channel and the Alborán Ridge. Along the northern part of the East Alborán sub-basin is Almería Fan, whose apex is at a depth of 1500 m and whose distal end is at a depth of 1850 m (Fig. 2).

2.5. 36º10'N High

The irregular outlined slightly convex northward Djibouti Trough is bordered on the south by a pear-shaped high we have tentatively named the 36°10′ high. Its outline is defined by the 900 m contour and its top is marked by seamounts on the west and Adra Ridge on the east (Fig. 2). East of 3°15′W, the 36°10′N high is nearly cut into two by a northwest-trending 9 km wide, 20 km long trough with a maximum depth of 1290 m (Fig. 2, Fig. 3). At its southeastward end, the trough, in the form of a hanging valley, terminates on a 400 m high northeast-trending scarp. Along the axis of the trough is a 1 km wide depression over 1000 m deep; the trough is flanked on its southwest side by a multipeaked 7.3 km long 6.5 km wide high defined by 875/900 m contours. Straddling this trough is a system of channels that drain into the Alborán Channel. Both the trough and the channel terminate westward on a system of northeast-trending lineation characterized by a chain of narrow depressions. The easternmost of these features extends across the 36°10′N and the Alborán Channel to merge with the northwest flank of the Alborán Ridge (Fig. 2). The southeast side of the 36°10′N high has a relief of 700–900 m, a gradient of 5–24° and is broadly convex to the northwest. This section of the high is deeply eroded by narrow gullies trending northwestward; this rough surface is onlapped by the sediments in the Alborán Channel (Figs. 4 and 5).

The 36°10′N is the sea floor expression of a horst, covered with Neogene volcanics and tilted northward (Fig. 2, Fig. 3; Watts et al., 1993; Comas et al., 1999). Drilling at DSDP site 121 at the west end of the 36°10′N high (Ryan et al., 1970; Le Pichon et al., 1971; Olivet et al., 1973; Campos et al., 1992; Maldonado et al., 1992) suggests that the high may have a core composed of metamorphic rocks of the Alborán Domain blanketed by Neogene volcanics. The features along the southeast edge of the 36°10′N high are related to recent strike slip motion along the normal fault-binding tilted horsts. A multi- channel seismic reflection profile recorded by Comas et al. (1995) across this irregular slope suggests that the country rock on this scarp consists of Alborán Domain (meta- morphic basement); possibly pre-rift and syn-rift sediments also may be present along the strike of the slope. These units are capped in places by Neogene volcanics, both of which in turn are covered by a discontinuous thin veneer of recent sediments.

[FIGURE 4]

2.6. Alborán Channel

The Alborán Channel is located between the 36°10′N high and the Alborán Ridge and links the West and East Alborán sub-basins (Fig. 2, Fig. 3). The floor of the channel deepens gradually to the northeast from a depth of 1500 m at its western end to 1800 m at its eastern mouth; its gradient ranges from <1° to 3°. East of B/O Vizconde de Eza Seamount the Alborán Channel is 20 km wide, at 3°15′W 3 km wide, north of Alborán Island 4 km wide, just east of 3°15′W, where the channel is constricted by a northeast-trending swell, 2 km wide, and at its eastern end 13 km wide. The floor of the channel is not as flat as previously suggested by Alonso and Maldonado (1992), but is disrupted by three small depressions. One of these lows extends from 3°15′W to 3°30′W, is aligned parallel to the channel's axis, has a relief of 100 m and a maximum depth of over 1700 m. The second depression, just east of 3°15′W, has a relief of >25 m and a maximum depth of >1650 m. East of 3°15′W the axis of the channel runs northeastward for a distance of 16 km to a third depression outlined by the 1850 m contour. From there the channel axis rises to a depth of less than 1850 m, from where it descends to a depth greater than 1850 m as it debouches onto the East Alborán sub-basin.

[FIGURE 5]

2.7. Alborán Ridge

Southeast of the Alborán Channel is the northeast-trending Alborán Ridge, which according to Woodside and Maldonado (1992) is the most distinct topographic feature of the Alborán Basin (Fig. 2, Fig. 3). The ridge is 150 km long and terminates on the southeast at approximately 4°1′W, 35°20′N on Xauen Bank west, shown in Fig. 2, Fig. 3 (Comas et al., 1995). Toward the northeast, the ridge terminates on the Habibas Escarpment. Illustrated in Fig. 2 is the 80 km northeast end of the ridge. Topographically, this segment of the ridge can be divided into three sections. Southwest of about 3°30′W the crest of the high is about 5 km wide, is defined by the 600 m contour and has a minimum depth of less than 282 m. This part of the ridge is separated from the

segment to the northeast by a 600 m deep less than 1.5 km wide saddle. Northeast of the saddle the Alborán Ridge crest is in the form of a platform with a maximum width of 7.5 km. Rising above this platform are the two small volcanic islands Alborán and Las Nubes and mound-like structures. The base of the Alborán Ridge northwest flank is at a depth of 1000/1100 m toward the southwest and 1400/1800 m toward the northeast. The base of the ridge's southeast flank is a depth of 1000 m toward the southwest and 1100 m toward the northeast end; the ridge's northeast end is in the form of a broad nose plunging northeastward.

The gradient of the northwest flank of the Alborán Ridge, the southeast margin of the Alborán Trough, ranges from 18° to as low as 1°. The northwest side of the ridge's platform segment is cut by gullies, most of which terminate on a bench at the base of the scarp that wedges out to the east. The shaded relief diagram gives an impression of bedding within the units resting on this bench that is truncated by the scarp (Fig. 4). The ridge's northwest flank also is indented by a northwest–southeast-trending embayment that penetrates deeply into the Alborán Ridge, nearly cutting it into two (Fig. 5).

The scarp on the southeast side of the Alborán Ridge is more linear than the one on its northwest side and has a gradient of 5–27° (Fig. 2, Fig. 3, Fig. 5). East of 2°45′W, this scarp and the ridge itself terminate on the Habibas Escarpment. Along the southeast scarp are 2 km-wide benches, one located at 3°15′W and the other at 3°07′W. At the base of the scarp also are presnt two irregular surfaced terrains, one near 3°W and the other at 3°10′W, with the latter extending to the crest of the Alborán Ridge (Fig. 3). Onlapping the southeast side of the Alborán Ridge also are three fans, one east of 3°15′W, another near 3°00′W and the third at 2°54′W. Feeding the last one is a canyon that can be traced to the edge of the platform at the crest of the Alborán Ridge. The fan at 3°00′W also is fed by a single canyon displaying a pronounced hook as it indents the edge of the platform on the ridge's crest. No canyon is associated with the fan at 3°15′W. We speculate that the mounds on the crest of the ridge represent deep-water coral mounds. We further suggest that the embayment on the northwest side of the ridge and the benches and chaotic terrain on the southeast side of the ridge are the creations of mass-wasting.

2.8. South basin apron

The Alborán Ridge, together with the Habibas Escarpment, forms the divide between the Alborán Basin's north and south basin aprons. The contact of the south basin apron with the southeast side of the Alborán Ridge is in the form of a 6–11 km wide trough, the South Alborán sub-basin (Fig. 2, Fig. 3). The floor of this basin dips gently northeastward with a gradient ranging from 3° to <1°. The low is in the form of a hanging valley with its eastern end being truncated by the southeast-trending Habibas Escarpment. The basin is asymmetrical in cross-section, with its 900 m high northwest side having a gradient of about 14°, whereas its 600 m high southeast side has a gradient of 4°. Its northwest side has the appearance of a fault scarp, but the topographic expression of its southeast side is one of a sediment rise whose edge is scarred by mass- wasting. Only the northeast end of this rise is included in our survey, but the topographic map in Maldonado et al. (1992) shows that the axis of the rise trends northeastward, with its southwest end abutting the north–south Melilla peninsula in North Africa. Dominating the part of the rise mapped during our survey are two north-trending highs, the 12 km wide, 22 km long West Cabliers Bank with a minimum depth of 350 m and the 22 km long 7 km wide Cabliers Bank with a minimum depth of 367 m. Separating the banks is the 30–22 km wide Cabliers Basin (Fig. 2). Submarine canyons cut the northern edges of both banks and the intervening basin.

2.9. Seamounts

2.9.1. Morphology

Topographic highs in the Alborán Basin have diameters ranging from about 1 km and reliefs of less than 100 m, more aptly defined as hills, to tens of kilometers long and wide such as the B/O Vizcone de Eza Bank, and reliefs of several hundred meters (Figs. 2 and 3). Many of the highs have irregular crests, but others are flat-topped, such as the Chella, Sabinar and Pollux banks. The eroded tops of these banks have served as foundations for biotherms probably composed of deep-water corals. Apparently, deep-water corals tend to concentrate in regions of tectonic uplift, such as the highs in the Alborán Basin (Hoernle et al., 2003). Many of the seamounts are partially

surrounded by circular outlined moats that seismic reflection profiles (Alonso and Maldonado, 1992; their Fig. 3) show are erosional in origin; they are probably due to bottom current activity. The multibeam data recorded during the present investigation verify such an interpretation.

A seamount with a minimum depth of 261 m and a diameter of 11 km and side slopes with a gradient of 10° occurs in the Malaga sub-basin. We have tentatively named this feature the Algarrobo Seamount (Fig. 2). A larger high, the east–west-trending 44 km long and 14 km wide Vizconde de Eza, with a minimum depth of less than 775 m and side slopes with a gradient of 21°, exists in the West Alborán sub-basin. Northwest of Vizconde de Eza Bank are two smaller highs, with the one near Vizconde de Eza having dimensions of 4×4.5 km and a minimum depth of <1050 m. The other high is 9.5×4 km, with a minimum of <1150 m and a relief of more than 150 m.

On the north basin apron southeast of Adra is the three-peaked Chella Bank (Fig. 6; Comas et al., 1992, Comas et al., 1999). Its 7.8 km2 flat top is 130 m deep at its southern end and 117 m at its northern end, its western flank has a declivity of 8° and its southeast one 18°. Resting on the erosional top is an irregular mass that reaches to a depth of 72 m. Northeast of Chella is another high that we have named ANE (Fig. 6; Afloramiento Nor-Este; Northeast Volcanic Exposure). This high consists of two banks linked by a narrow high. In contrast to the flat-topped Chella, the top of ANE consists of a series of trending northwest–southeast linear highs. Separated from Chella by a nearly 290 m deep erosional low on the west is another high that we have named AW (Fig. 6; Afloramiento Oeste; West Volcanic Exposure). The trend of the crest of this high is north–south at its southern end, but turns abruptly to northwest–southeast at its northern end, where it appears to be linked with a northwest-trending fracture. Between Chella and AW are at least 12 circular protrusions of probable volcanic origin. We infer that the linear highs associated with ANE are probably fault controlled and the northeast-trending lineation linked to NW probably is a northwest-trending right-lateral fault. We further speculate that the irregular mass capping Chella Bank probably represents carbonate build-up by deep-water corals.

[FIGURE 6]

On the basin's lower slope off Cabo de Gata are the Sabinar and Pollux banks and two narrow ridges (Fig. 2, Fig. 3). Sabinar is a twin peaked bank. Its west peak is 9 km long and 3.2 km wide, with its crest at a depth of 252 m and its sides having a maximum gradient of 21°. It is separated from the east peak by a l 2.4 km long low with a maximum depth of 615 m. The east Sabinar peak is 10 km long and 3.5 km wide, with a minimum depth of 264 m and maximum slope declivities of 22°. The north-trending Pollux Bank also is a twin-peaked bank, with the crest of the west peak less than 347 m deep and that of the east peak having a minimum depth of 273 m and its slopes having maximum gradients of about 15°.

On the north side of the East Alborán sub-basin is a semi-circular high with a diameter of 14.5 km, a minimum depth of 1415 m and maximum slope declivities of about 11°. It is linked to the base of the lower slope off Cabo de Gata by a northeast trending swell divided into two by a saddle over 1575 m deep. This feature is generally referred to as the Maimónides Ridge, but its shape suggests that the term seamount is more appropriate (Fig. 2, Fig. 3). Mauffret et al. (1992) described the seamount as a volcanic structure superimposed on a broad tilted block, supposedly the swell connecting the seamount to the base of the lower slope. Mauffret et al. also stated that the southern side of the seamount displays a zig-zag pattern, but no such pattern is indicated by the multibeam data. The pattern displayed by this slope is more of an embayed one. Along the southern side of the East Alborán sub-basin is the less than 1500 m deep Yusuf Ridge, a north of west-trending high bordered on its southern side by an over 1900 m deep narrow depression. Beyond the depression is the 500–600 m high Habibas Escarpment with a declivity as high as 9°.

The western end of the 36°10′N high (Fig. 2, Fig. 3) is dominated by three large seamounts whose side slopes have gradients of 10–22°. We have tentatively named two of these features the North and South Herradura seamounts (Fig. 2, Fig. 3). South Herradura has a diameter of 17 km; its flat-top crest is at a depth of 273 m and its base is at a depth of about 800 m. North Herradura is somewhat squarest in outline, has a crestal depth of 422 m and its base is at a depth of 800 m. The Djibouti Bank is defined by the 800 m contour along its southern side and 650 m contour at its northern side (Fig. 2, Fig. 3). Its peak displays a minimum depth of 231 m and has side slopes

gradients of 17°. Southeast of the bank, there is a 1.9 km wide northeast-trending trough with a maximum depth of 880 m. Southeast of the trough are three small highs with minimum depths of 347–494 m (Fig. 2, Fig. 3). On the east edge of the 36°10′N high are five other northwest-trending highs named the Adra Ridge by Estrada et al. (2000). Depths along their crests varied from 578 to 825 m.

2.9.2. Origin

The seamounts in the Alborán Basin have two origins: the uplifted Alborán basement and Miocene volcanism (Gierman et al., 1968; Mauffret et al., 1987; Alvarez- Marrón, 1999). Dredging by Hoernle et al. (2003) on the B/O Vizconde de Eza Bank, which they call Ibn Batouta Seamount, demonstrated that this bank consists not of volcanic rocks but of metasediment and gabbroic rock, probably an amphibole gabbro, a composition indicative of the Alborán Domain (one of four tectonic pre-Miocene domains involved in the Gibraltar Arc; the others are the Iberian Paleomargin, African Paleomargin and the Flysch Trough; see Fig. 1). The three small highs northwest of B/O Vizconde de Eza Bank (Fig. 2) and the Adra Ridge at the east end of the 36°10′ high also may have the same origin, but this has to be verified by sampling.

2.10. Submarine canyons

Submarine canyons and channels in the Alborán Basin are found on the basin's north slope, the east side of Djibouti Trough and the flanks of the Alborán Trough and Ridge and Habibas Escarpment (Fig. 3). The canyons on the basin's north slope, west of Cabo de Gata, extend some distance onto the basin's apron before dying out, whereas the erosional features on the east side of the Djibouti Trough, Alborán Ridge and Trough and Habibas Escarpment are generally limited to the scarps. In those along the southeast side of the Alborán Ridge, some of the canyons display amphitheatre-like heads. These like features, like those on the canyons off New Jersey (Pratson and Coakley, 1996), are the creations of repeated small- scale mass-wasting processes.

2.10.1. North basin slope

We have grouped the submarine canyons on the basin's north slope into five systems: the Fuengirola (Ercilla et al., 1992), Almuñeecar, Motril, Calahonda, Campo de Dalías and Almería canyon systems (Fig. 3). According to Alonso and Ercilla (2003), the rivers feeding many of these systems are of similar length, 69–96 km, and drain areas of about the same size of 1258–1915 km2. The Fuengirola system on the west drains into the West Alborán sub-basin, the Almuñecar, Motril and Calahonda systems into the Djibouti Trough and those in the Gulf of Almería into the East Alborán sub-basin (Fig. 3).

The Fuengirola System, supposedly fed now or in the past by Río de Fuengirola, displays a simple geometry consisting of a meandering trunk valley that cuts into the shelf's edge and can be traced to a depth of 1100 m (Fig. 3). The main canyon is sinuous and has a length of about 33 km and a relief ranging from about 100 m at its head to less than 10 m at its mouth. A distributary splaying from the main channel at 36°20′N has topographic expression to a depth of about 950 m.

The Almuñecar System associated with Rio Verde consists of five short valleys that can be mapped to a depth of about 600 m with lengths ranging from 4 to 13 km, reliefs in the order of tens of meters and widths of several km (Fig. 7).

Alonso and Ercilla (2003) described the Motril System as consisting of two 3 km long canyons with widths of 1.5–1 km and reliefs of 185–1.5 km that display meanders with an average sinuosity of 1.2 (Fig. 7). Alonso and Ercilla (2003) report that the canyons change down slope into channels that can be traced to 850 m water depth. These channels in turn change into merging lobe deposits forming a 1.4 km wide fan. Our data suggest that the eastern branch breaks into a series of distributaries at a depth of 775 m and that one of these branches merges with the western branch at a depth of 875 m. Our data further suggest that the meanders in both branches are associated with slumps and that the canyons are deeply entrenched onto the outer shelf, with the branches being formed by the confluence of several small canyons at the shelf's edge.

[FIGURE 7]

The Calahonda System consists of 12 sinuous to slightly curved to rectilinear valleys whose heads indent the shelf's edge (Fig. 7). The canyons have reliefs of 124–90 m at their heads to 21–2 at their distal ends. Widths range from 1 km to 250 m at their heads and from 180 to 400 m at their mouths, and lengths range from 17 to 1 km. The locations and shape of some of the canyons are influenced by normal faults oriented obliquely to the shelf's edge. The canyons on the east side of the system originate at the base of scarp on the upper basin slope, whereas those in the in the center and eastern sides of the system cut across the scarp. A canyon on the east side of the system is asymmetrical in cross-section, with its eastern side being formed by a curved steep scarp and its western side having a much gentler slope. The canyon diminishes in relief down the slope sharply and appears to have been formed by two cycles of erosion: an older one consisting of a broadly undulating thalweg and a younger one deeply entrenched on the older one. The younger canyon is limited to the upper slope, whereas the older one extends on to the basin's apron.

Within Almería Bay, there are two canyon systems, Campo de Dalías on the west and Almería Canyon on the east side of the bay (Fig. 8). The canyons of the Campo de Dalías Canyon system initiate seaward of the shelf's edge; most of them do not indent the shelf break (Fig. 8). In plan view, the canyons are rectilinear to slightly curved, have lengths ranging from 17 to about 4 km, widths ranging from 630 to 150 m at their heads and 470 to 130 m at their distal ends and reliefs ranging from 26 to 1 m at their heads and 11 to 1 m at their distal ends. The main feature of these canyons is their right-slip lateral displacement by the seaward extension of the northeast-trending left-lateral Serrata-Carboneras fault system (Fig. 8). Not all the canyons, however, are displaced by the fault or show the same magnitude of displacement.

[FIGURE 8]

If these canyons are related to any drainage in the Campo de Dalías plain, they must be to the ''ramblas'' (ephemeral arroyos) in the plain, not the Andarax River. This system is too wide to be due to drainage from a single river and the Andarax River is too far east of the system to have contributed detritus that created the turbidity currents that eroded the canyons (Fig. 8). That the canyons do not cut onto the shelf and their wide distribution along the upper slope suggest that

they were eroded by turbidity currents triggered by fault activity on the upper slope, an activity documented by the zig-zag pattern displayed by the shelf's edge in plan view. We infer that the displacement by the canyons as they cross the Serrata-Carboneras Fault is not structurally controlled because, if it did, it means that the Serrata-Carboneras changes from left-lateral onshore to right-lateral offshore. Bell et al. (1997) stated that movement along the inshore section of the fault during the last 100 ka has been of vertical uplift rather than strike-slip. We infer that motion along the offshore extension was the same, with the vertical motion being documented by a northwest-facing scarp along the southeast side of the fault trace. We further speculate that the channels entering the fault trace are younger than 100 ka. Thus, as the channels entered the fault trace, they were deflected in a right-lateral sense before they returned to their original orientation of flow. Thus, these valleys are deflected and not offset valleys and are not indicative of the direction of relative fault displacement (Keller and Pinter, 2002).

The most striking of the canyons in Almería Bay is Almería Canyon (Fig. 8). This canyon is known by two names, Almería Canyon (Medialdea Vega et al., 1982; Cronin, 1994, upgraded in the Internet in 2000; Alonso and Ercilla, 2003; Marıín et al., 2003) and Andarax Canyon (Cronin et al., 1995). We prefer the name Almería Canyon for its location in the bay of that name rather than Andarax as the head of the canyon is not near this river, but is off the Rambla de Morales. The tributaries of Almería Canyon originating off the Campo de Dalías drain nearly south and are deflected by the Serrata-Carboneras Fault as they cross the fault before draining into the Almería Canyon. The tributaries draining into the Almería Canyon System from the northeast originate in Sierra de Gata. The main tributary of the Sierra de Gata is broadly curved as it debouches onto the Almería Canyon (Fig. 8). The origin of this curvature is yet to be resolved. It could be of structural or due lithologic changes in the country rock along the canyon's course.

Almería Canyon has a topographic expression to a depth of about 80 m and indents the outer shelf in Almería Bay (Fig. 8; Medialdea Vega et al., 1982). North of 36°35′N the valley parallels the seaward extension of the La Serrata-Carboneras fault zone and is aligned northeast–southwest, but south of about 36°30′N, southwest of Sabinar Bank, the channel turns southerly and then

southeasterly. As noted by previous investigators (Cronin, 1994; Cronin et al., 1995; Alonso and Ercilla, 2003; Marín et al., 2003) and us, the channel beyond the canyon mouth at about a water of 1200 m is a meandering channel with steep side slopes with gradients of 15°.

The multibeam data collected during the present investigation show slumps and slump scars, some of which form terraces, projecting onto the channel of the Almería Canyon (Fig. 8). Many of these slump terraces are associated with the channel meanders, suggesting that the meanders were formed as a result of the turbidity currents being deflected by them. The present investigation also indicates that the lower reach of Almería Canyon is dominated by a fan—the Almería Fan—whose head is defined by a 1400 m contour and its distal end by a 1900 m contour (Fig. 8). The fan fills the low extending from Maimónides Seamount to the base of the Habibas Escarpment. Apparently, this scarp forced the turbidity currents eastward, depositing their load at the western end of the East Alborán sub-basin. The northern edge of the fan appears to be onlapped or onlaps the sediments displaced from the slope south of the Pollux and Sabinar banks. These displaced sediments were partially dammed by the northern slope Maimónides Seamount, but the bulk of the sediment drained around the seamount to onlap the Almería Fan (Fig. 8). Sediments also may have been contributed to the Almeria Fan from the south. A canyon on the West Cabliers Bank can be traced to the crest of the Habibas Escarpment, where it dies out at a depth of 1200 m. A canyon on the east side of the Cabliers Bank dies out at a depth of 1300 m on the crest of the Habibas Escarpment and the one on the west side of the bank extends to a depth of 1350 m. Sediments may also have originated from the Cabliers Basin between the two banks, as the north slope of this basin is scarred by mass-wasting processes as it descends to the crest of the Habibas Escarpment at a depth of 1200 m.

2.10.2. East slope of the Djibouti Trough and south side of the 36º10'N high

A system of northwest-trending 9–20 km long, <1 to 1 km wide and tens of meters deep gullies occur on the east slope of the Djibouti Trough and on the south side of the 36°10′N high (Fig. 3,

Fig. 4, Fig. 5). Their topographic continuity is disrupted by one circular depression that probably represents a pockmark formed by the expulsion of gas (see below). The southeast of the Serrata-Carboneras Fault extends to the base of the slope descending to the East Alborán Sub-Basin. Those in the 36°10′N high are connected to the northwest-trending lows cutting the southeast edge of the 36°10′N high, where rocks of the Alborán Domain (one of the four pre-Miocene tectonic domains involved in the Gibraltar Arc; García-Dueñas et al., 1992) are exposed. We infer that submarine sedimentary processes created these features. Their dimensions and orientation oblique to the supposed westerly flowing Mediterranean led us to eliminate the possibility that they represent furrows (1–150 m wide, 0.5–350 m deep and hundreds of meters long; see Flood, 1983) eroded by bottom currents. We suggest that they were formed of turbidity currents or sheet debris flows. Those cutting across the Alborán Domain along the southeast edge of the 36°10′N probably are the result of headward erosion and represent superposed channels that acquired their courses on sediments resting on the Alborán Domain. The channels later cut through the sediments transected the buried Alborán Domain and acquired their courses independent of the structure of the domain.

2.11. Pockmarks and mounds

Pockmarks, circular to ellipsoidal craters, with tens of meters in diameter and reliefs of less than 5 m, were mapped on the basin slope off Cabo de Gata, at the apex of the Almería Fan, the western edges of the Alborán Channel, the 36º10'N high, in the center of the high, northwest of the North Herradura Bank and in the vicinity of the Algarrobo Bank. Two examples of such pockmarks are imaged in Fig. 4. We infer that they are due to the seepage of gas (thermogenic or biogenic) and interstitial fluids from the underlying sediments along the fracture zones.

The most interesting features encountered during the present investigation are three fields of mounds (Figs. 9 and 10). Two of these fields are located east of Malaga at the base of the upper slope at a water depth of 225–250 m. The other is located southwest of the Campo de Dalias, north and northwest of the Chella Bank, at a depth of 150–225 m. The mounds have reliefs of 1–9 m and lengths of 91–131 m. On TOPAS seismic reflection profiles, the mounds have smooth

outlines, with one of the larger structures being indented at its top as though having a crater. In both profiles the acoustic impendence of the mounds is such as to obscure the deeper acoustic stratigraphy. Whereas reflectors beneath the mounds in the vicinity of Málaga appear to be continuous beneath the mounds, those off Campo de Dalias are faulted (Figs. 9 and 10). The mound orientation in the vicinity of Chella Bank ranges from northwest, parallel to the upper slope, to slightly east of north at an oblique angle to the slope. The mounds near Málaga have an unusual distribution being concentrated around a structurally controlled spur at the shelf edge. The features in the vicinity of Chella Bank are made of two groups, those to the northwest and southeast appear subdued as though they are partially buried, whereas those in the center are quite sharp in the shaded relief diagram. Those in the vicinity of Malaga also display similar grouping, with the ones on the west being circular and having the appearance of being partially buried. The ones east of Malaga look like small rods, whereas the smaller mounds northwest of Chella Bank are sub-circular, but the larger ones are elongate and have the appearance of chains of beads made up of four to as many as six of the circular structures. In the absence of ground truth (images and samples), we are unable to discern the origin of these features. As the mounds tend to rest on an undisturbed horizon (Fig. 1), a diapiric or mud volcanic origin for these features can be rejected. As they rest on a bottom easily penetrable by the low-energy TOPAS seismic profiler, we also have discounted the possibility that the structures represent deep-coral mounds, as these structures develop on hard ground (see O'Reilly et al., 2003). Thus, we have tentatively inferred that the mounds may represent carbonate structures. If so, the carbonates were probably precipitated from the oxidation of methane by bacteria and are comparable to the features described by Camoin et al. (1988) and Canet et al. (2003). The structures are the consequence of expulsion and oxidation of methane supported by the acoustic wipeouts along Line 164 in Fig. 10. However, in the absence of ground truth, this interpretation has yet to be verified.

[FIGURE 9]

[FIGURE 10]

2.12. Bottom currents

The presence of the moats surrounding the seamounts, the irregular seafloor of the Alborán Channel, and the extensive exposure of basement (Alborán Domain) along the southern edge of the 36º10'N high have led us to infer that bottom currents have played and are playing a role in the creation of the seafloor morphology of the Alborán Basin. However, some of the areas lacking sediment cover, particularly in steep slopes, may be the result of a deficiency in sediment supply or a downslope displacement.

2.13. Faults

The shaded relief map in Fig. 3 and the 3-D map in Fig. 11 allow one to appreciate the nature and extent of linear topographic features on the Alborán Basin. These features, which are limited to the part of the Alborán Basin east of 3°40′W, have three topographic expressions, scarps, narrow linear furrows and ridges and a chain of small rectangular to lenticular depressions. We infer that all these features are the expressions of faulting and folding, and as these dislocations affect the sea floor, they are of recent geologic age. The faults display four trends: east–west, northeast–southwest and west of north and northwest, and affect the sea floor, indicating that they are active or have been active in the recent past (Fig. 3). In a companion paper (Ballesteros et al., in press), we discuss the significance and origin of these structures.

2.14. Mass wasting

Features that resemble mass-wasting are common in the Alborán Basin, with most having two origins, faulting or volcanism or both. Others are the result of repeated small- scale mass-wasting processes at the head of submarine canyons. Some of these features are very large, covering an area of 20 x 20 km in the South Alborán sub-basin, and those off Cabo de Gata have dimensions ranging from 20 x 9 to 3 x 4 km (Fig. 8). Mass-wasting also is quite extensive along the northwest slope of the Alborán Channel with the features having dimensions of as much as 15 x 5 to 3 x 3 km. Fault-associated slides also occur along the southeast scarp of the Alborán Ridge and have dimensions in the order of 15 x 4 to 9 x 7 km. Mass- wasting structures associated with volcanic

structures and B/O Vizconde de Eza, a metamorphic basement high, range from embayments created by slumping/debris flows to irregular topography. We infer that the irregular topogra- phy on the northwest side of the Alborán Ridge between 2°40′W and 3°0′W was formed by creep or thin slides (Fig. 3). Embayments along the bases and upper slope of seamounts formed by gravitational processes range in size from 2 x 2 km to features whose dimensions are in the order of tens of km.

[FIGURE 11]

3.CONCLUSIONS

The morphology of the Alborán Basin as imaged by multibeam bathymetry and the shaded relief and 3D diagrams constructed from these data is the creation of several discrete events. The first of these events was the Miocene-rifting phase, during which the continental crust underwent massive thinning and created the 36°10′N high and the B/O Vizconde de Eza Bank. Concurrent with this rifting was the Miocene volcanism that was responsible for the formation of the seamounts scattered over the surface of the basin and the Alborán Ridge. The second creative phase that took place is associated with the post-rift basinward sediment progradation leading to the formation of the basin margins and aprons. The third event is one of faulting related to the continuing convergence of the Eurasian and African plates, a compressional phase that began in the latest Miocene and is still taking place today, producing folding, strike-slip faulting and inversion of rift structures. This faulting led to the uplift of the center and margins of the basin, the triggering of mass-wasting and turbidity currents on the basin slopes and sides of topographic highs within the basin. We infer that most of the features of the Alborán Basin are the result of these tectonic events. More recent events that contributed to the basin morphology are bottom currents that eroded the moats surrounding the seamounts and the floor of the Alborán Channel and kept the southern edge of the 361100N high sediment free, expulsion of gas and fluids that constructed the mounds at the base of the north slope and excavated circular depressions,

pockmarks, throughout the basin and the Pleistocene glacially induced regressions/ transgressions. As a result of these changes in sea level, the basin area shallower than 120 m experienced cycles of erosion and deposition. Migration of the shoreline to the shelf's edge and shift of the depocenter to the outer shelf and upper slope also led to the intensification of turbidity current activity on the basin slope and apron, leading to the formation of a submarine canyon on the basin margins.

Acknowledgments

We express our appreciation to the Captain and crew of B/O Vizconde de Eza during the cruises, Secretaría General de Pesca Marı´tima (SGPM) for providing ship-time in the frame of the ''Cartas de Pesca Project'' and Instituto Español de Oceanografía for technical and financial support.

References

Alonso, B., Ercilla, G., 2003. Small turbidite systems in a complex tectonic complex setting (SW Mediterranean): Morphology and Growth Patterns. Marine and Petroleum Geology 19, 1225–1240.

Alonso, B., Maldonado, A., 1992. Plio-Quaternary margin growth patterns in a complex tectonic setting: northeast Alborán Sea. Geo-Marine Letters 12, 137–143.

Alvarez-Marrón, J., 1999. Pliocene to Holocene structure of the eastern Alborán Sea (western Mediterranean). In: Zahn, R., Comas, M.C., Klaus, A. (Eds.), Proceedings of Ocean Drilling Program, Scientific Results, vol. 161. College Station, Texas, pp. 345–555.

Ballesteros, M., Rivera, J., Muñoz, A., Muñoz-Martín, Acosta, J., Carbó, A., Uchupi, E., in press. Alborán Basin, southern Spain. Part II: tectonics. Marine and Petroleum Geology, doi:10.1016/j.marpetgeo. 2007.05.004.

Bell, J.W., Amelung, F., King, G.C.P., 1997. Preliminary late Quaternary slip history of the Carboneras Fault, southeastern Spain. Journal of Geodynamics 24, 51–66.

Campos, J., Maldonado, A., Campillo, A.C., 1992. Post-Messinian evolutional patterns of the Central Alborán Sea. Geo-Marine Letters 12, 173–178.

Camoin, G., Bernet-Rollande, M.C., Philip, J., 1988. Rudist-coral-framed works associated with submarine volcanism in the Maastrichtian of the Pachino area (Sicily). Sedimentology 135, 123–138.

Canet, C., Prol-Ledesma, R.M., Melgarejo, J.C., Reyes, A., 2003. Methane-related carbonates formed at submarine hydrothermal springs; a new setting for microbially-derived carbonates. Marine Geology 199, 205–242.

Comas, M.C., Dañobeitia, J.J., Álvarez-Marrón, J., Soto, I., 1995. Crustal reflections and structure in the Alborán basin: preliminary results of the ESCI–Alborán survey. Rev. Soc. Geol. España 8 (4), 75–88.

Comas, M.C., García-Dueñas, V., Jurado, M.J., 1992. Neogene tectonic evolution of the Alborán Sea from MCS data. Geo-Marine Letters 12, 157–164.

Comas, M.C., Platt, J.P., Soto, J.I., Watts, A.B., 1999. The origin and tectonic history of the Alborán basin: insights from Leg 161 results. In: Zahn, C., Comas, M.C., Klaus, A. (Eds.), Proceedings of the Ocean Drilling Program, Scientific Results, vol. 161. College Station, Texas,

pp. 555–580.

Cronin, B.T., 1994. Channel-fill architecture in deep-water sequences: variability, quatification and applications. PhD Thesis, University of Wales, 332pp.

Cronin, B.T., Kenyon, N.H., Woodside, J., den Bezemer, T., van der Wal, A., Millington, J., Ivanov, M.K., Limonov, A., 1995. Views of the Andarax submarine canyon: a meandering system on an active tectonic margin. In: Pickering, K.T., Hiscott, R.N., Kenyon, N.H., Ricci, R., Smith,

R.D.A. (Eds.), Atlas of Deep Water Environments—Architectural Style in Turbidity Systems. Chapman & Hall, London, pp. 84–88.

Emery, K.O., 1960. Basin plains and aprons off southern California. Journal of Geology 68, 469–479.

Ercilla, G., Alonso, B., Baraza, J., 1992. Sedimentary evolution of the northwestern Alborán Sea. Geo-Marine Letters 12, 144–149.

Estrada, F., Ercilla, G., Alonso, B., 2000. El sistema turbidítico de Almería y el noroeste del Mar de Alborán: evolución tectosedimentaria durante el Plio-Cuaternario. In: Valles submarinos y sistemas turbidíticos modernos. Alonso, B., Ercilla, G. Eds., CSIC. Barcelona. Parte I: Sistemas turbidíticos, pp. 113–134.

Flood, R.D., 1983. Classification of sedimentary furrows and a model for furrow initiation and evolution. Geological Society of America Bulletin 94, 630–639.

García-Dueñas, V., Balanyá, J.C., Martínerz-Martínez, J.M., 1992. Miocene extensional detachments in the outcropping basement of the northern Alborán Basin (Betics) and their tectonic implications. Geo-Marine Letters 12, 88–95.

Gierman, G., Pfannenstiel, M., Wimmenauer, W., 1968. Relation entre morphologie tectonique et volcanisme en mer d'Alborán (Mediterranée occidentale). Comptes Rendus Sommaire del Societe Geologique des France 4, 116–118.

Heezen, B.C., Tharp, M., Ewing, M., 1959. The floors of the oceans; 1. The North Atlantic. Geological Society of America Special Paper 65, 122pp.

Hernández-Molina, F.J., Somoza, L., Rey, J., 1996. Late-Pleistocene– Holocene high resolution sequence analysis on the Alborán Sea continental shelf. In: De Batist, M.M., Jacobs, P. (Eds.), Geology of Siliceous Shelf Seas, vol. 117. Spec. Publ. Geol. Soc. London, pp. 139–154.

Hoernle, K., 25 others, 2003. Ostatlantik Mittlelmeer-Schwarzes Meer. Part 1. Cruise No. M51, Leg 1. 12 September–15 October 2001, Warnemünde-Málaga. Meteor-Beriche 03-1, 38pp.

Keller, E.A., Pinter, N., 2002. Active Tectonics. Earthquakes, Uplift, Body, and Landscape, second ed. Prentice-Hall, Upper Saddle River, NJ, 362pp.

Le Pichon, X., Pautot, G., Auzende, J.M., Olivet, J.L., 1971. La Méditerranée occidentale depuis l0Oligocene. Sche´ma d0e´volution. Earth Planetary Science Letters 13, 145–152.

Maldonado, A., Campillo, A.C., Mauffret, A., Alonso, B., Woodside, J., Campos, J., 1992. Alborán Sea Late Cenozoic tectonic and stratigraphic evolution. Geo-Marine Letters 12, 179–186.

Marín, M.A., Grácia, E., Soto, J.I., Blodel, P., Geomez-Sichi, O., HITS Cruise Party, 2003. Tectonic control on the sedimentary architecture of the Almería margin (Alborán Sea: high-resolution imaging; abs.). International Conf. Deep Water Processes in Modern and Ancient Environments., Barcelona & Ansia 28, 15–19.

Mauffret, A., El-Robrini, M., Gennesseaux, M., 1987. Indice de la compression re´cente en mer Mediterranée: un basin losangique sur la marge nord-algérienne. Bulletin de la Societe Geologique de France 6, 1195–1206.

Mauffret, A., Maldonado, A., Campillo, A.C., 1992. Tectonic framdework, of the Eastern Alborán and Western Algerian basins, western Mediterranean. Geo-Marine Letters 123, 104–110.

Medialdea Vega, J., Baena Pérez, J., García Rodríguez, J., Maldonado, A.E., Uchupi, E., Udías Vallina, A., Wandossell, J., 1982. Mapa geológico de la plataforma continental española y zonas adyacentes. E: l:200,000. Almería-Garrucha. Chella-Los Genoveses. Instituto Geológico y Minero de España, 105pp.

Olivet, J.-L., Pautot, G., Auzende, J.-M., 1973. Alborán Sea. In: Ryan, W.B.F., Hsu, K.J., et al. (Eds.), Initial Reports of the Deep Sea Drilling Project, vol. X111. US Government Printing Office, Washington, DC, pp. 1417–1430.

O'Reilly, B.M., Readman, P.W., Shannon, P.M., Jacob, A.W.B., 2003. A model for the development of a carbonate mound population in the Rockall Trough base down deep-towed sidescan sonar data. Marine Geology 198, 55–66.

Pratson, L.F., Coakley, B.J., 1996. A model for headwall erosion of submarine canyons induced by downslope-eroding sediment flows. Geological Society of America Bulletin 108, 225–234.

Ryan, W.B.F., Stanley, D.J., Hersey, J.B., Fahlquist, D.A., Alla, T.D., 1970. The tectonics and geology of the Mediterranean Sea. In: Maxwell, A.E. (Ed.), The Sea, vol. 4. Wiley-Interscience, New York, pp. 387–492.

Watts, A.B., Platt, J.P., Buhl, P., 1993. Tectonic evolution of the Alborán basin. Basin Research 5, 153–177.

Woodside, J.M., Maldonado, A., 1992. Styles of compressional neotectonics in the Eastern Alborán Sea. Geo-Marine Letters 12, 111–116.

FIGURE CAPTIONS

Fig. 1. Geologic setting of the Alborán Basin region. AG=Águilas; AL=Almería; MA=Málaga; CA=Cádiz; GR=Granada; SE=Sevilla; T=Tangier; ML=Melilla. Modified from Vegas (1992). 1=Neogene basins and volcanics; 2=Alborán Domain; 3=Iberian Paleomargin; 4=African Paleomargin; 5=Flysch; 6=Paleozoic basement.

Fig. 2. Bathymetric chart of the Alborán Basin compiled from multibeam acquired during the present investigation. Contour interval 50 m, color change every 200 m.

Fig. 3. Shaded relief map of the Alborán Basin compiled from multibeam data. See Fig. 2 for names of prominent topographic features. AI=Alborán Island; AL=Almuñecar Canyon System; AM=Almería Canyon System; C=Calahonda Canyon System ; F=Fuengirola Canyon System; D=Dalías Canyon System; M=Motril Canyon System; SC=Serrata-Carboneras Fault.

Fig. 4. Shaded relief map of the northwest side of the Alborán Ridge in the vicinity of Alborán Island, the Alborán Channel and the southeast flank of the trough. View looking northwest. Points of interest are the gullies (G), bench (B) and suggestion of bedding on the northwest scarp of the Alborán Ridge, the irregular surface of the sediment fill on the Alborán Channel (AC) suggestive of bottom currents, the gullies (G) on the 36°10′N High (H) and the slumps (SL) on the southeast side of the Alborán Ridge. AI=Alborán Island; AR=Adra Ridge; F=fault; P=pockmark.

Fig. 5. Shaded relief map of the embayment (E) on the northwest side of the Alborán Ridge. We infer that this feature is due to massive collapse of the sediments onlapping the Alborán Ridge volcanic core. AI=Alborán Island; AC=Alborán Channel; B=bench; F=fault; G=gullies; H=36°10′N High; S=South Alborán sub-basin; SL=slumps. Rough terrain on the northwest side of the AC images exposure of Alborán Domain, a pre-Miocene tectonic domain involved in the Gibraltar Arc (García-Dueñas et al., 1992).

Fig. 6. (A) Shaded relief map of Chella Bank compiled from multibeam data. (B) Geomorphic interpretation of A. CH=Chella Seamount; SC=slump scar; ANE=Afloramiento Nor-Este

(Northeast Volcanic Exposure); AW=Afloramiento Oeste (West Volcanic Exposure); Black pattern=volcanic protrusions; F=fault.

Fig. 7. Shaded relief map of Almuñecar (AL), Motril (M) and Calahonda (C) canyon systems. Compiled from multibeam data. A=artifact; F=fault; GR=Graben.

Fig. 8. Shaded relief map of Dalías Canyon system (D) and Almería bay Canyon (AC) system and tributaries. Compiled from multibeam data. Note the displacement of tributaries from Campo de Dalias by the left-lateral Serrata-Carboneras Fault (SC) that appear to have been displaced right-laterally along the shear. Note that one of the Almería canyon northeast tributaries also is disrupted by northwest-trending right-lateral faults. AF=Almería Fan; CGB=Cabo de Gata Bank; CH=channel; F=fault; HE=Habibas escarpment; LLS=lower lower slope; M=Maimónides seamount; PB=Pollux Bank; SB=Sabinar Bank; SC=Serrata-Carboneras Fault; SL=scars of slumps and debris flows; ULS=upper lower slope. Note that the upper and lower slopes south and southwest of Cabo de Gata Bank display extensive evidence of mass-wasting and that the basin apron at the foot of the slope consists of debris flows and turbidites.

Fig. 9. Shaded relief map (A) and TOPAS seismic reflection profile (B) of mounds off Malaga. F=fault; US=upper slope. The linearity of the upper slope suggests that it is fault controlled.

Fig. 10. Shaded relief map (A) and TOPAS seismic reflection profile (B) of mounds in the vicinity of Chella Bank. AW=acoustic wipeouts due to presence of gas, F=fault; US=upper slope; ANE=Afloramiento Nor-Este (Northeast Volcanic Exposure); A=artifacts; white numbers=water depth in meters.

Fig. 11. 3-D diagram of Alborán Basin compiled from multibeam data. View looking southwest. AB=Algarrobo bank; AC=Almería Canyon; AI=Alborán Island; AR=Adra Ridge; CB= Cabliers Bank; CH=Chella Bank; DB=Djibouti Bank; DT=Djibouti Trough; EASb=East Alborán sub-basin; H=36°10′N High; HE=Habibas Escarpment; SASb=South Alborán sub-basin;

WASb=West Alborán sub-basin; VEB=B/O Vizconde de Eza Bank; WC=West Cabliers Bank; YR=Yusuf Ridge.

FIG.1

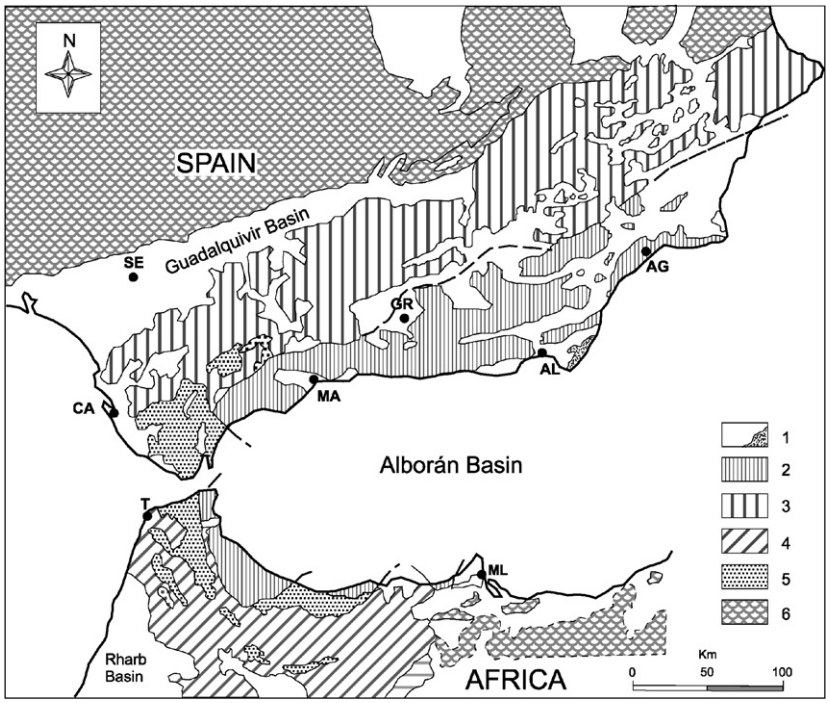
N
SPAIN
Guadalquivir Basin
SE
AG
GR
AL
MA
CA
Alborán Basin
T
ML
Rharb
Basin
AFRICA
1
2
3
4
5
6
Km
0
50
100

FIG. 2

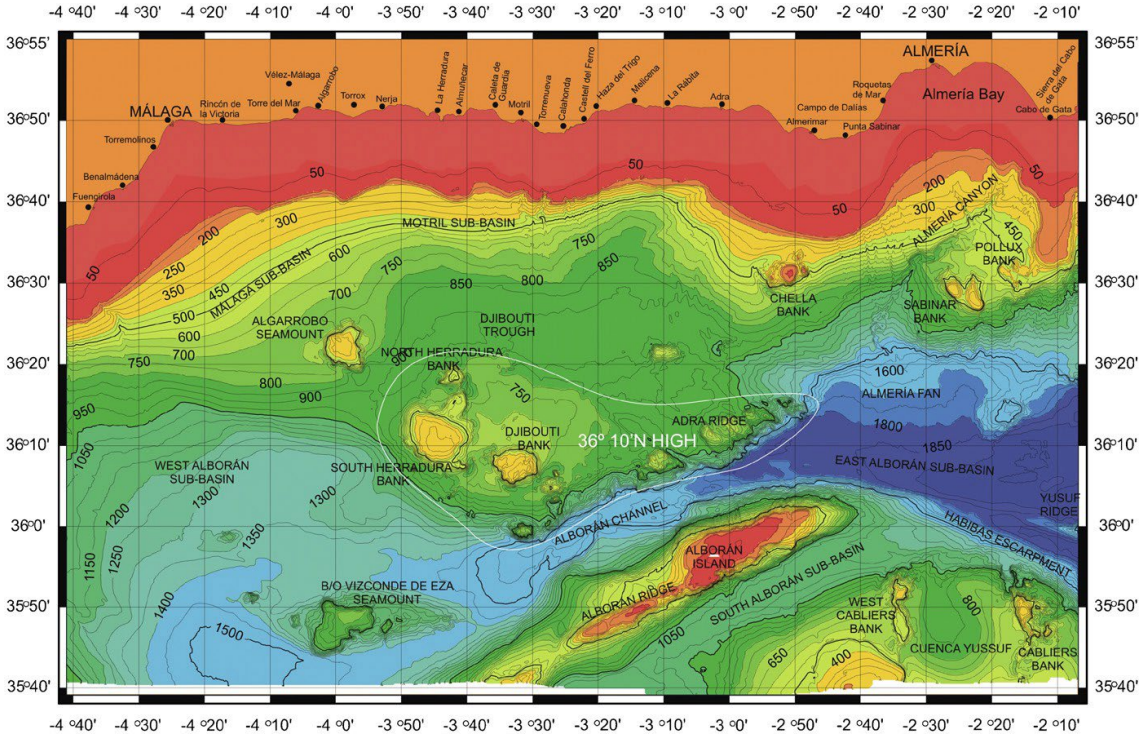
-4 °40'
-4 °30'
-4 °20'
-4 °10'
-4 °0'
-3 °50'
-3 °40'
-3 °30'
-3 °20'
-3 °10'
-3 °0'
-2 °50'
-2 °40'
-2 °30'
-2 °20'
-2 °10'
36°55'
36°50'
36°40'
36°30'
36°20'
36°10'
36°0'
35°50'
35°40'
MÁLAGA
Vélez-Málaga
Rincón de la Victoria
Torre del Mar
Algarrobo
Torrox
Nerja
La Herradura
Almuñécar
Calaba de Calahonda
Motril
Torrenueva
Castell del Ferro
Haza del Trigo
Melicena
La Rábita
Adra
Campo de Dalías
Almerimar
Roquetas de Mar
Punta Sabinar
ALMERÍA
Almería Bay
Sierra del Cabo de Gata
Cabo de Gata
Torremolinos
Benalmádena
Fuengirola
MOTRIL SUB-BASIN
MÁLAGA SUB-BASIN
ALMERÍA CANYON
POLLUX BANK
CHELLA BANK
SABINAR BANK
ALGARROBO SEAMOUNT
DJIBOUTI TROUGH
NORTH HERRADURA BANK
ALMERÍA FAN
ADRA RIDGE
DJIBOUTI BANK
36° 10'N HIGH
WEST ALBORÁN SUB-BASIN
SOUTH HERRADURA BANK
EAST ALBORÁN SUB-BASIN
YUSUF RIDGE
ALBORÁN CHANNEL
HABIBAS ESCARPMENT
ALBORÁN ISLAND
B/O VIZCONDE DE EZA SEAMOUNT
ALBORÁN RIDGE
SOUTH ALBORÁN SUB-BASIN
WEST CABLIERS BANK
CUENCA YUSSUF
CABLIERS BANK

FIG. 3

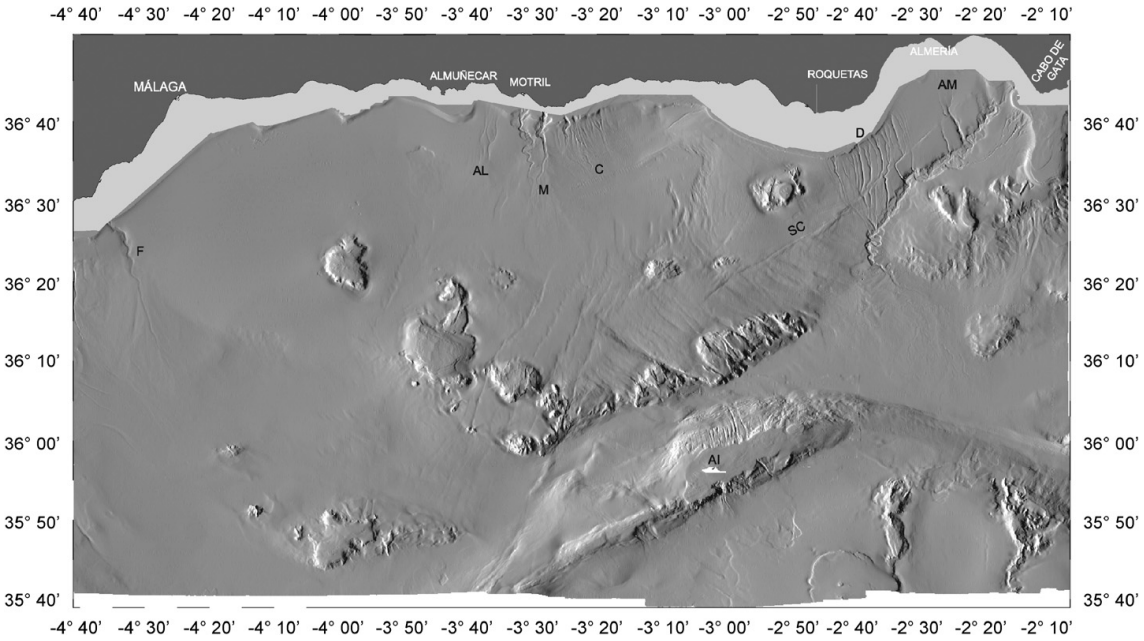
-4° 40' -4° 30' -4° 20' -4° 10' -4° 00' -3° 50' -3° 40' -3° 30' -3° 20' -3° 10' -3° 00' -2° 50' -2° 40' -2° 30' -2° 20' -2° 10'
MÁLAGA
ALMUÑECAR
MOTRIL
ROQUETAS
ALMERIA
CABO DE GATA
AM
D
AL
M
C
SC
F
AI
36° 40'
36° 30'
36° 20'
36° 10'
36° 00'
35° 50'
35° 40'

FIG. 4

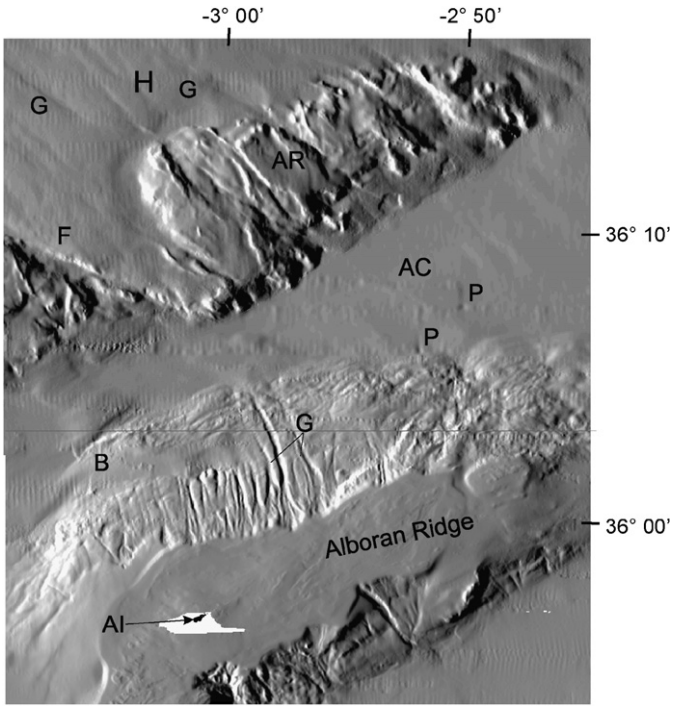

FIG. 5

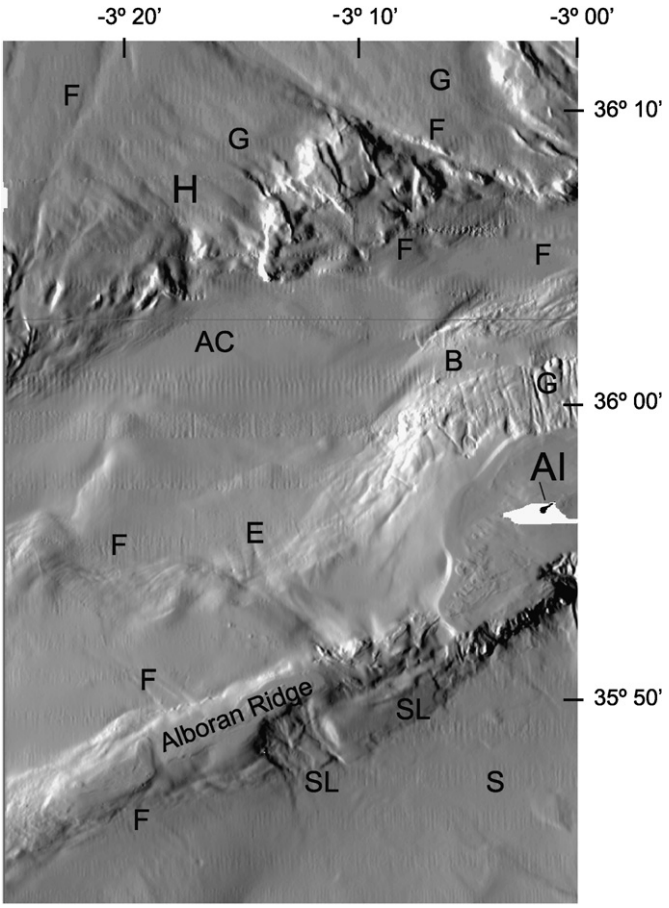
-3º 20'
-3º 10'
-3º 00'
36º 10'
36º 00'
35º 50'
F
G
H
AC
B
E
Al
Alboran Ridge
SL
S

FIG. 6

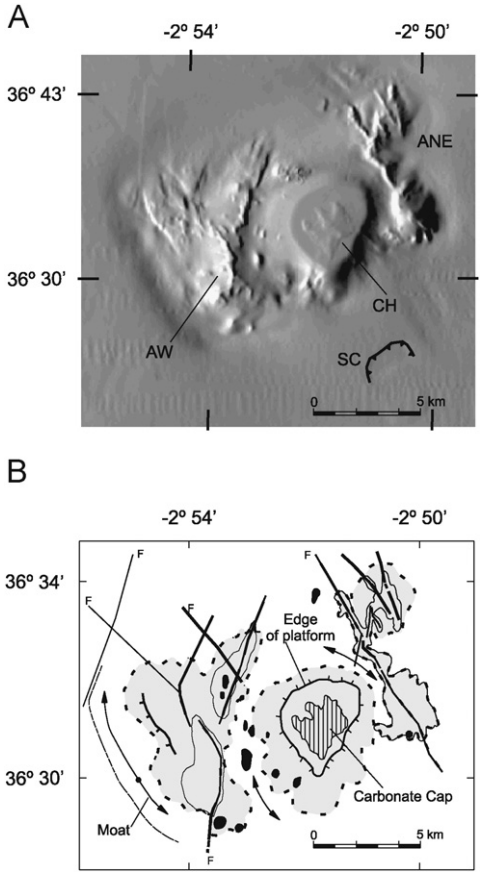
A
-2° 54'
-2° 50'
36° 43'
36° 30'
ANE
CH
AW
SC
0
5 km
B
-2° 54'
-2° 50'
36° 34'
36° 30'
F
Edge
of platform
Carbonate Cap
Moat
0
5 km

FIG. 7

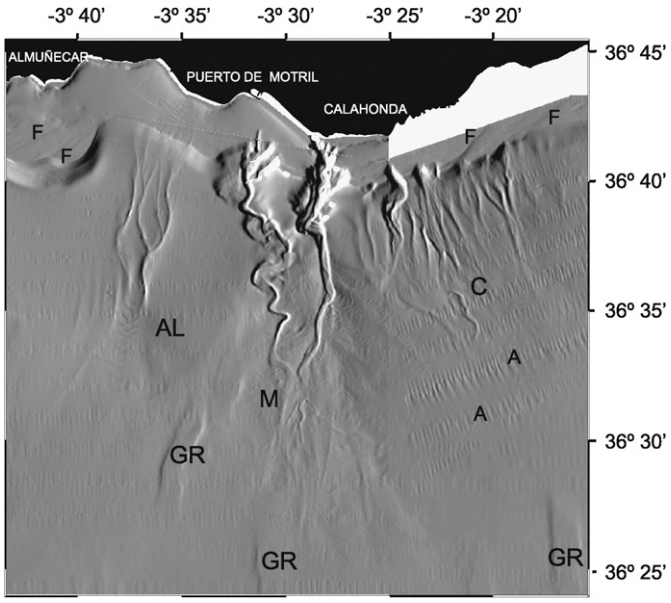
-3º 40'
-3º 35'
-3º 30'
-3º 25'
-3º 20'
36º 45'
36º 40'
36º 35'
36º 30'
36º 25'
ALMUÑECAR
PUERTO DE MOTRIL
CALAHONDA
F
F
F
F
C
AL
A
M
A
GR
GR
GR

FIG. 8

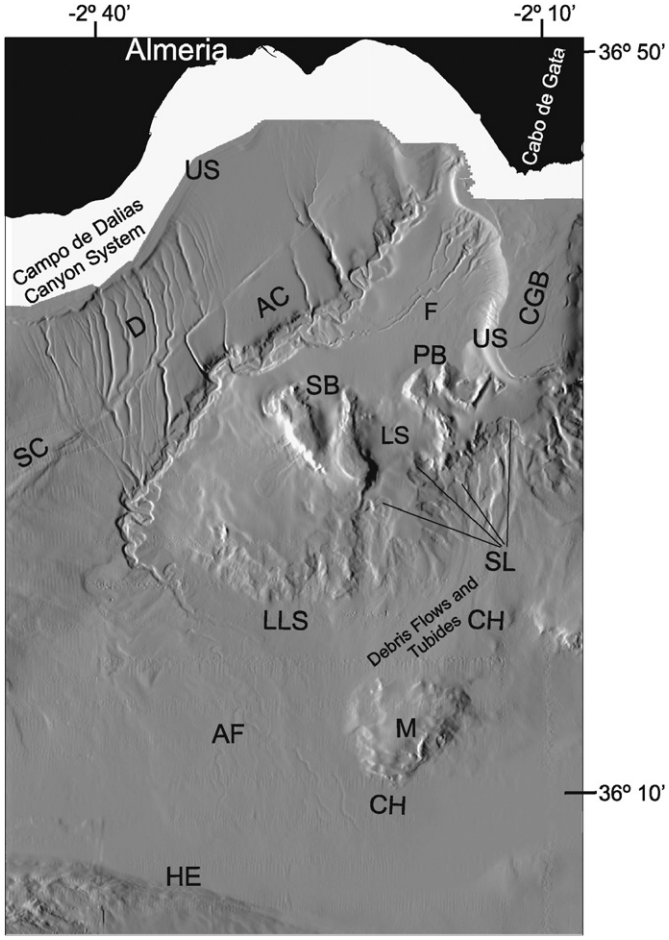
-2º 40'
-2º 10'
Almeria
Cabo de Gata
36º 50'
US
Campo de Dalias
Canyon System
D
AC
F
CGB
US
PB
SB
SC
LS
SL
LLS
Debris Flows and
Tubides
CH
AF
M
CH
36º 10'
HE

FIG. 9

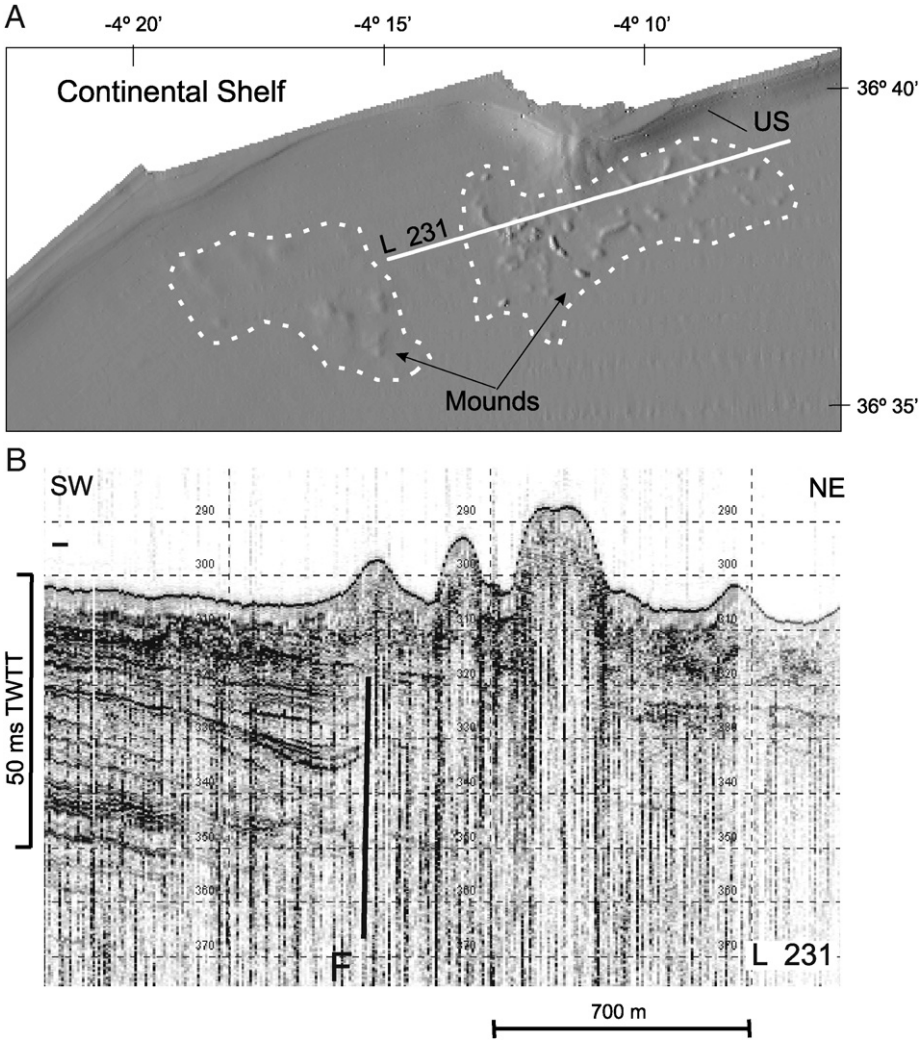
A
-4° 20'
-4° 15'
-4° 10'
Continental Shelf
36° 40'
US
L 231
Mounds
36° 35'
B
SW
NE
50 ms TWTT
L 231
700 m

FIG. 10

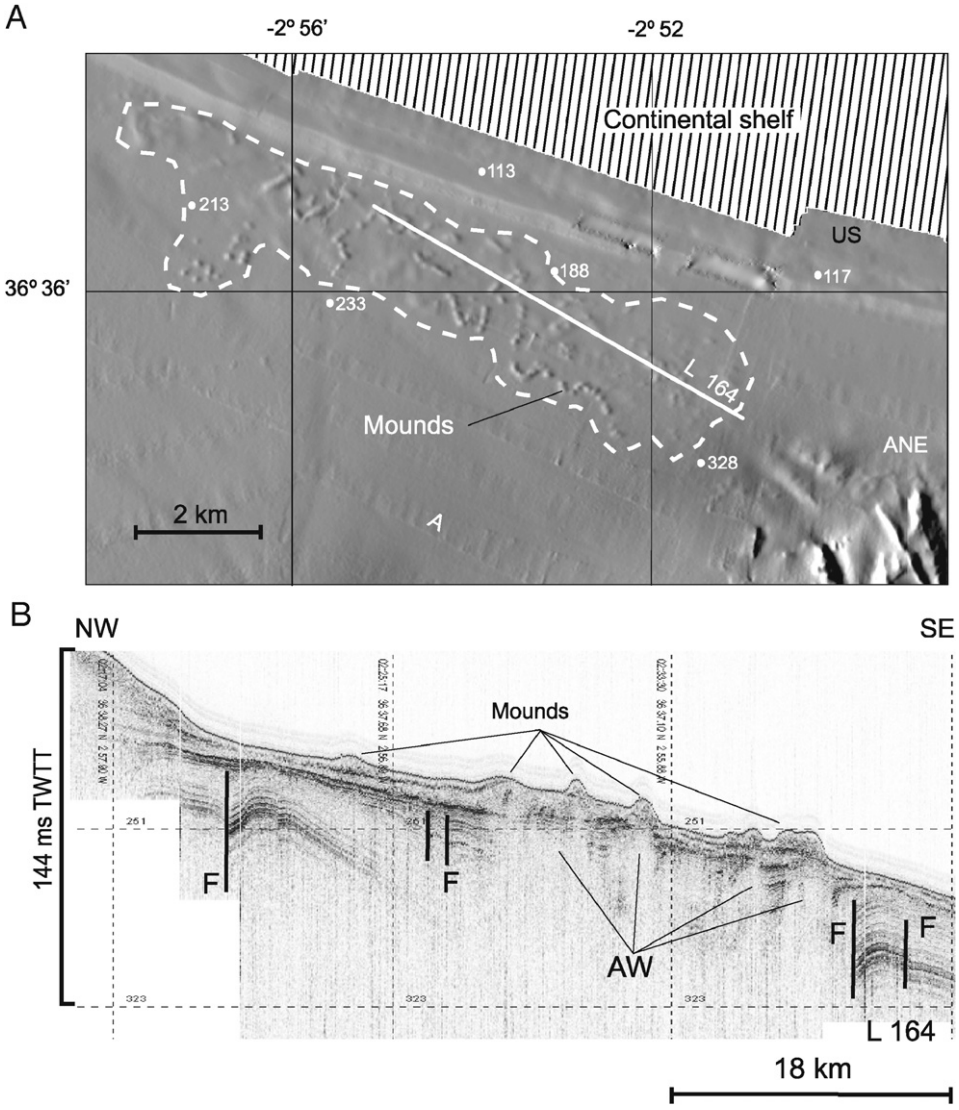
A
-2º 56'
-2º 52
Continental shelf
113
213
188
117
US
36º 36'
233
L 164
Mounds
ANE
328
2 km
A
B
NW
SE
144 ms TWTT
Mounds
F
F
AW
F
F
L 164
18 km

FIG 11

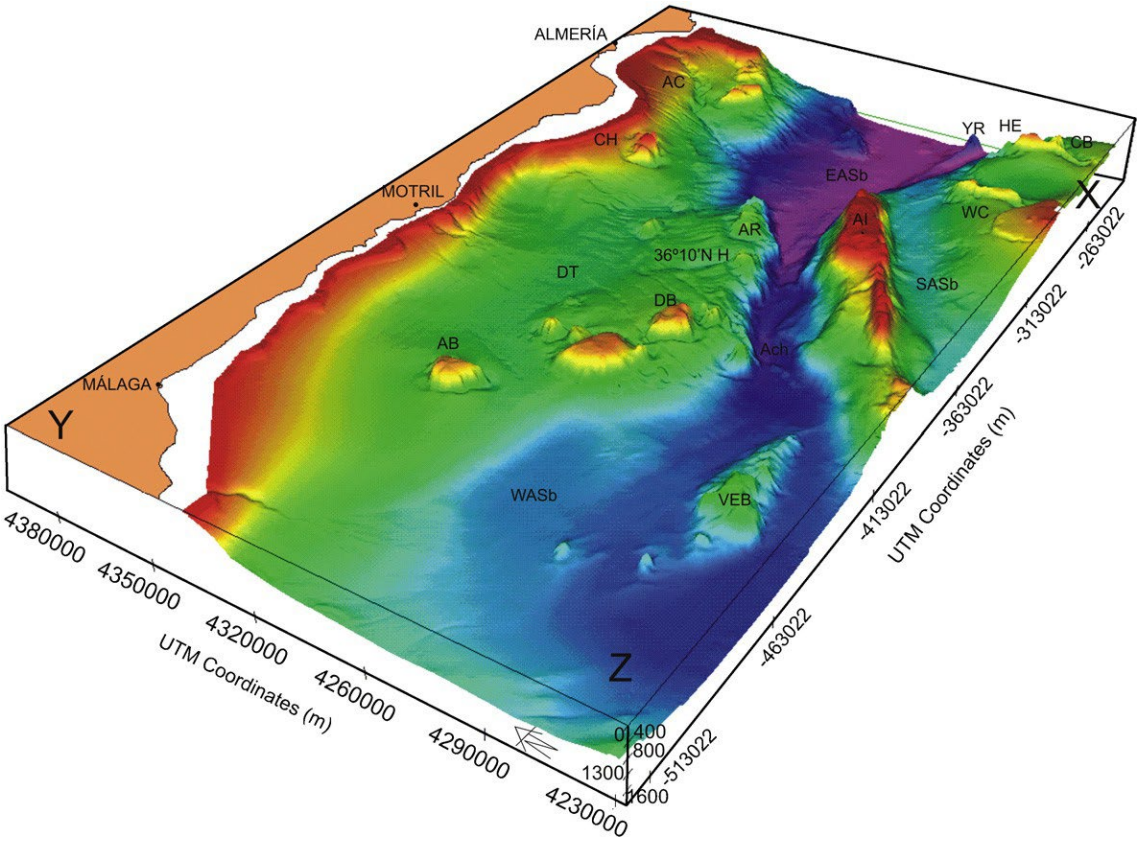
ALMERÍA
AC
CH
MOTRIL
YR
HE
CB
EASb
WC
AR
AI
36°10'N H
DT
SASb
DB
AB
Ach
MÁLAGA
Y
WASb
VEB
X
-263022
-313022
-363022
-413022
-463022
-513022
UTM Coordinates (m)
4380000
4350000
4320000
4260000
4290000
4230000
UTM Coordinates (m)
Z
0
400
800
1300
1600